

# Simple fiber-optic refractive index sensor based on evanescent higher order modes

Jiahua Chen\*, Wojtek J. Bock, Predrag Mikulic

Centre de recherche en Photonique, Département d'informatique et d'ingénierie, Université du Québec en Outaouais, P.O. Box 1250, Gatineau, Québec, J8X 3X7 Canada

## ABSTRACT

This paper presents an optical fiber refractive index sensor based on the evanescent higher order modes. Its structure and principle are quite simple. The sensor is composed of two segments of optical fibers that are spliced together. An ordinary multimode fiber with a core diameter of 50  $\mu\text{m}$  is used to input the light. The functions of a second multimode fiber with a core diameter of 200  $\mu\text{m}$  are twofold. In the region of the splice, a section of the cladding a few centimetre long is removed by an electrical discharge. This part works as a sensing element, and the rest of the fiber is used to output the light. Once the light travels through the input fiber and crosses the splice to enter the second fiber, numerous modes both guided and leaky are generated due to the abrupt increase of the core diameter. The evanescent light fields of these guided modes are sensitive to changes in the refractive index of the material surrounding the fiber cladding. The evanescent field change directly causes a change in the output light intensity. The developed sensor is compact in size, simple to fabricate, promising in performance, and has a high potential for practical applications.

**Keywords:** Refractive index sensor, Fiber-optic, Evanescent, Higher order mode

## 1. INTRODUCTION

A variety of devices and approaches have been developed to measure refractive index. In some optical fiber devices, the light in the fiber can leak into its environment or the light energy in the fiber can be transferred to the environment through the evanescent field. The degree of leakage or the amount of energy transferred varies with changes in the environment. This property can be used to determine the refractive index of the gas or liquid materials surrounding the fiber and thus to form a fiber refractive index sensor. Fiber-optic refractive index sensors have numerous advantages over conventional devices including easy fabrication, simple structure, compact size, relatively high accuracy and significant potential for environmental and biochemical monitoring. So far, several kinds of fiber refractive index sensors, most of them using ordinary fibers, have been studied and developed. Among the technologies employed in recent designs are the following: hetero-core (or core diameter mismatch) [1][2][3][4], core-offset [5], fiber Bragg grating [6][7][8], long-period grating (LPG) [9][10][11], fiber laser [12], and several others [13] [15][16]. The techniques that have been applied include: thin metal film coating to get a surface plasmon resonance (SPR) [2][4][13], thin film overlay coating [10], reduction of the cladding diameter [6][8][14], and short wavelength diffraction in the case of a photonic crystal fiber [17]. None of these technologies is simple. The core-offset structure needs a careful adjustment of the offset level; a cladding reduction approach requires a precise control of the cladding diameter; the fiber Bragg gratings, the LPGs, and the fiber lasers are not easy to fabricate in an ordinary lab; and depositing a coating metal film or an overlay is also a precise and generally time-consuming work. Ultimately, the hetero-core or the core diameter mismatch seems the simplest structure [1][3] and this is what we have used in our design. This paper presents a simple yet very advantageous optical fiber refractive index sensor design that is supported by promising measurement results.

## 2. SENSOR STRUCTURE AND SENSING PRINCIPLE

An optical fiber FT-200-UMT is a commercial multimode fiber with a large core diameter (200  $\mu\text{m}$ ) and a thin cladding layer (cladding diameter of 225 $\mu\text{m}$ ). The unique property of this fiber is that the thin cladding can be removed without any damage to the fiber core. This is a major advantage for our sensing application based on the evanescent higher order modes. According to the instructions of the manufacturer, the cladding can be rubbed away with a soft paper soaked with

\*jiahua.chen@uqo.ca; phone 1 819 595-3900 ext 1619; fax 1 819 773-1638

acetone. Actually it is quite difficult to entirely remove this cladding in this way especially when just a short part of the fiber is concerned. In the developed sensor, a short part of the jacket was removed mechanically, the thin cladding layer was removed by an electrical discharge, and then the fiber part with its cladding removed was spliced to an ordinary multimode fiber (core diameter of 50  $\mu\text{m}$ ) that is used for inputting light as shown in Fig. 1.

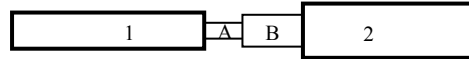


Fig. 1. Sensor structure: 1 - multimode fiber with cladding diameter of 125  $\mu\text{m}$ ; 2 - multimode fiber with core diameter of 200  $\mu\text{m}$ ; A - fiber part without jacket; B - fiber part without cladding.

The light modes traveling in fiber segment 1 are guided. The corresponding light rays can be either meridional or non-meridional. The path of a non-meridional ray is confined between two concentric cylinders: the outer cylinder is the core-cladding interface and the inner cylinder is situated between the interface and the fiber axis. Once the light enters part B of fiber segment 2, the light modes will change suddenly due to the abrupt change of the fiber core size. A large amount of light modes both leaky and guided are then generated in fiber segment 2. The former will partially escape out and cause loss, while the latter will be still guided but will be affected by various factors such as fiber bending and changes in the core diameter. Fig. 2 depicts a simple situation of light transmission through a core-core interface. The guided light in fiber segment A travels towards the right, then crosses the interface of the two fiber ends, and finally enters fiber segment B. Every light dot in the core-core interface can be regarded as a new light source that emits meridional and non-meridional light rays into fiber segment B, except for one dot at the center of the second fiber that emits only meridional rays. The emitting light can be divided into two types: guided and leaky. Both can be either meridional or non-meridional. For the sake of simplicity, let us consider the meridional rays. In Fig. 2 the light rays emitted from point J and within angle  $\Omega$  are guided rays that can be detected at the end of fiber segment B, and the rest are leaky modes that contribute to some loss.

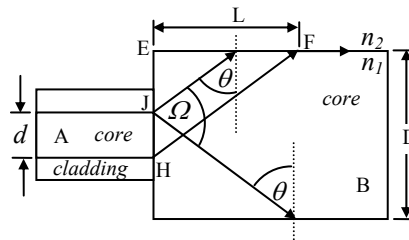


Fig. 2. Meridional rays in the sensing part: A - input fiber; B - output fiber;  $d$  - core diameter of the input fiber;  $D$  - core diameter of the output fiber;  $n_1$  - refractive index of the core of fiber B;  $n_2$  - external refractive index;  $\theta$  - critical angle determined by  $n_1$  and  $n_2$ ;  $\Omega$  - angle in which the emitting rays will be guided; J and H – the end points of the core-cladding interface.

For the given fibers A and B, the distance  $L$  between points E and F is a function of refractive index  $n_2$  of the material surrounding fiber segment B. This implies that a different surrounding material will cause a different light loss and hence that by measuring the output light intensity, one can gain some information about the surrounding material.

### 3. EXPERIMENT AND RESULTS

The measurement set-up is shown in Fig. 3. The light emitted from the broadband light source LS is guided by a multimode fiber (core diameter of 50  $\mu\text{m}$ ). It is then launched into the sensor to be tested through a connector. The output light from the sensor is collected by a multimode fiber (core diameter of 400  $\mu\text{m}$ ) that is connected to an optical spectrum analyzer (OSA) of Ocean Optics USB2000. Finally the output signal is input through a USB cable into a computer for processing. The spectrum of the signal is displayed on the screen.

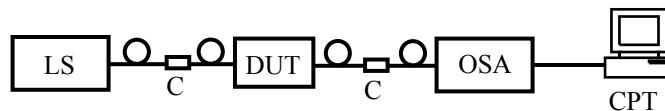


Fig. 3. The measurement set-up: LS – light source Mikropack DH-2000 UV-VIS-NIR; DUT - device under test; C - connector; OSA - optical spectrum analyzer Ocean Optics USB2000; CPT - computer.

For such a sensor surrounded by air or by an aqueous solution, the output spectrum is determined by the light source and by the injection conditions of the input light. Fig. 4(a) shows the output spectrum curves of a sensor in which the sensing part was surrounded by air and Glycerine solutions. The top curve is the output spectrum of the sensor in air. The separation between the curves is due to the different percentages of Glycerine in distilled water that create different refractive indices and hence represents a measurement of such refractive index differences. Figs. 4(b) and 4(c) are, respectively, the outputs for solutions of Glycerine and Ethylene Glycol, normalized to eliminate the influences of the light source and the light injection conditions.

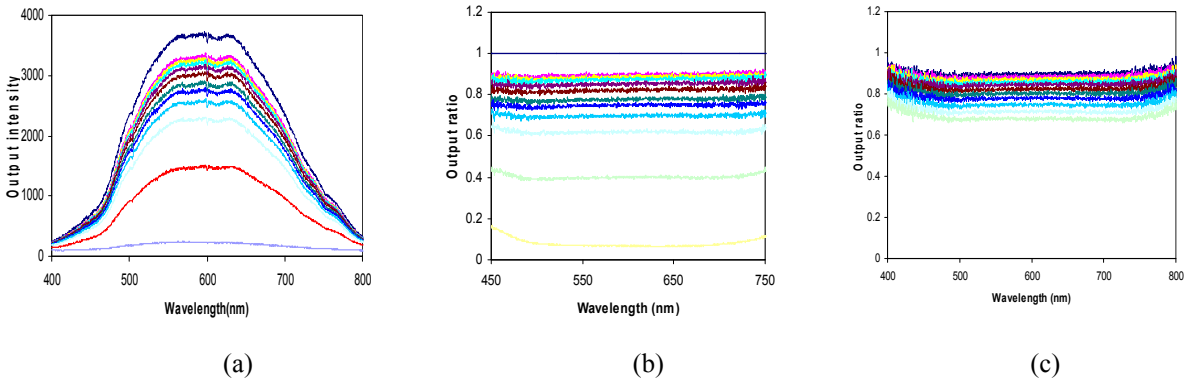


Fig. 4. The output spectrums of the sensor: (a) non-normalized (Glycerine); (b) normalized (Glycerine); (c) normalized (Ethylene Glycol). Curves from top to bottom: air, 0, 10, 20, 30, 40, 50, 60, 70, 80, 90, 100% of solvent in water.

The normalized outputs versus the refractive index are shown in Fig. 5. It can be seen that the resolution of the sensor varies with the refractive index: it is higher near the refractive index of the core and becomes lower near that of the water. The sensor is not particularly effective for liquids whose refractive indices are similar to that of the fiber core of FT-200-UMT, but improves for a higher refractive index contrast.

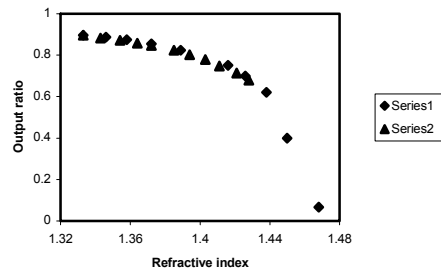


Fig. 5. The output ratios for solutions of Glycerine and Ethylene Glycol versus their refractive indices: Series 1 - Glycerine; Series 2 - Ethylene Glycol.

#### 4. DISCUSSION

Figs. 6(a) and 6(b) illustrate the intensity patterns of the output light of the sensor projected onto a screen without and with the surrounding Glycerine. The distance between the end of the output fiber and the screen is about 8 mm. The camera was fixed during the process of picture taking. The cladding of the end part of the output fiber was removed by discharge, so that the output light came out directly from the core of the FT-200-UMT fiber. It is clear from these pictures that the light spot is bigger and brighter when the sensor is in the air and it becomes smaller and darker when the sensing part is surrounded by Glycerine. The diminishing of the spot size of the output light visible on the screen is due to the escape of both the non-meridional rays and the meridional rays in that region, while the weakening of the intensity of the remaining part of the light spot is mainly caused by the escape of the meridional rays. The shadowed part in Fig. 6(c) illustrates the smaller light spot as observed on the screen after Glycerine is applied to the sensor. It should be noted that the annular part is not proportional to that on the fiber end. In reality the latter is a little smaller.

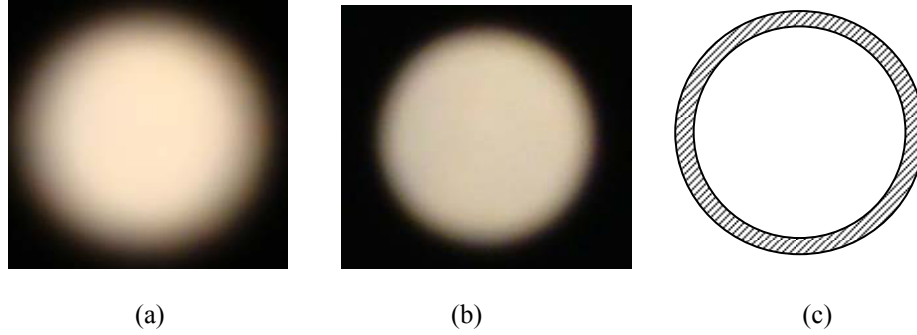


Fig. 6. Output light spots and their sizes: (a) sensing part surrounded by air; (b) Sensing part surrounded by Glycerine; (c) spot size comparison.

For a given refractive index  $n_2$  ( $n_2 < n_1$ ) of a surrounding liquid, the length  $L$  in Fig. 2 is determined by:

$$L = \frac{n_2}{2\sqrt{n_1^2 - n_2^2}}(d + D) \quad (1)$$

For water and assuming  $d=50 \mu\text{m}$ ,  $D=220 \mu\text{m}$ ,  $n_1=1.457$ , and  $n_2=1.333$ , the length  $L$  can be calculated as  $306.0 \mu\text{m}$  according to Eq. (1). The sensing distance of the sensor for the meridional rays is thus theoretically less than half a millimeter. Actually the experiment reveals that the sensing length is much longer than that. It is in fact about 18 mm. This implies that in the experiment, the rays most responsible for the light loss occurring in the fiber FT200-UMT are skew rays whose paths in the guiding fiber are helical, i.e., so called meridional rays. The actual measurements were done with a sensor having its sensing part 25 mm long and its measurement results showed little difference from that obtained with a sensor whose sensing length is 18 mm.

Fig. 5 indicates that the resolution of the sensor is not uniform but it increases with the refractive index. The lowest resolution is near the refractive index of 1.33. An experiment was done to determine what would be the resolution of the sensor towards the left side of the output curve. The results are shown in Table 1: the sensor can distinguish the refractive indices of the solutions of the Ethylene Glycol at percentages of 2, 3, 4, and 5%, but cannot distinguish them at percentages of 0 and 1.

Table 1. Ethylene Glycol percentage (0~5%) – Refractive index – Sensor output ratio.

Percentage (%)	Refractive Index	Normalized Ratio
0	1.3331	0.89623
1	1.3340	0.89644
2	1.3352	0.89536
3	1.3364	0.89389
4	1.3371	0.89344
5	1.3383	0.89217

It can be seen from Figs. 4(b) and 4(c) that the normalized output spectrum in the range of  $550 \sim 670 \text{ nm}$  is nearly a horizontal line especially for the solutions of Ethylene Glycol. Clearly, the sensor is wavelength-independent in this range. This implies that the choice of the light source for the sensor is much easier. In principle, any source can be used if its output spectrum is within that flat region, but actually an LED would be the best choice. For such a light source there is no wavelength at which the output notch exists. An OSA is thus not necessary as a decoding instrument. It could be replaced with a light intensity detector or an optical power meter. This property, together with the short sensing

segment needed (less than 30 mm) could make the whole sensing system very compact and economic. Fig. 7 shows the measurement results obtained with an hp 8152A average power meter.

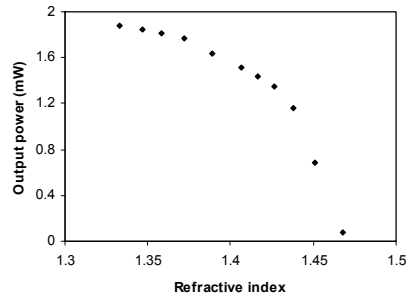


Fig. 7. Output power for different solutions of Glycerine

If  $n_1$  is equal to or higher than  $n_2$ , no guided mode could exist in the fiber; Eq. (1) is no longer valid. But in the latter case, the sensor can still work to some extent. Fig. 8 shows the output spectrum for Glycerine and for instrument oil with a refractive index of 1.482.

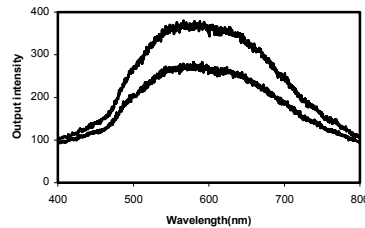


Fig. 8. Output spectrum for Glycerine and for instrument oil: upper curve - Instrument oil; lower curve - Glycerine

The output of this sensor results primarily from the fact that the light can be partially reflected by the boundary of the core and the solution, and guided by the fiber. The light modes in the output fiber are leaky ones.

If a thin metal layer is deposited onto the surface of the fiber, it becomes an SPR sensing element that can also be used to sense changes in the refractive index of the material surrounding the metal surface. Among the advantages of the sensor described here over such an SPR sensor are the following: no need of a metal film, no need of an OSA, and no need to determine the minimum position of the output spectrum.

## 5. CONCLUSIONS

An optical fiber refractive index sensor has been developed successfully. Its structure and principle are quite simple yet it has numerous advantages including: compact size, simple structure, easy fabrication, promising performance, and significant potential for a number of practical applications.

## ACKNOWLEDGEMENT

The authors gratefully acknowledge support for this project from the Natural Sciences and Engineering Research Council of Canada and from the Canada Research Chairs program.

## REFERENCES

- [1] Iga M., Seki, A., Kubota, Y., and Watanabe K., "Acidity measurements based on a hetero-core structured fiber optic sensor," *Sensors and Actuators B*, 96, 234-238 (2003).
- [2] Iga, M., Seki, A., and Watanabe, K., "Hetero-core structured fiber optic surface plasmon resonance sensor with silver film," *Sensors and Actuators B*, 101, 368-372 (2004).
- [3] Villatoro, J. and Monzon-Hernandez, D., "Low-cost optical fiber refractive-index sensor based on core diameter mismatch," *Journal of Lightwave Technology*, 24, 1409-1413 (2006).
- [4] Iga, M., Seki, A., and Watanabe, K., "Gold thickness dependence of SPR-based hetero-core structured optical fiber sensor," *Sensors and Actuators B*, 106, 363-368 (2005).
- [5] Tian, Z., Scott, S-H. Yam, S. S-H., and Loock, H-P., "Single-mode fiber refractive index sensor based on core-offset attenuators," *IEEE Photonics Technology Letters*, 20(16), 1387-1389 (2008).
- [6] Iadicicco, A., Campopiano, S., Cutolo, A., Giordano, M., and Cusano, A., "Self temperature referenced refractive index sensor by non-uniform thinned fiber Bragg gratings," *Sensors and Actuators B*, 120, 231-237 (2006).
- [7] Liang, W., Huang, Y., Xu, Y., Lee, R. K., and Yariv, A., "Highly sensitive fiber Bragg grating refractive index sensors," *Applied Physics Letters*, 86, 151122-1-151122-3 (2005).
- [8] Huang, X-F., Chen, Z-M., Shao, L-Y., Cen, K-F., Sheng, D-R., Chen, J., and Zhou, H., "Design and characteristics of refractive index sensor based on thinned and microstructure fiber Bragg grating," *Applied Optics*, 47(4), 504-511 (2008).
- [9] Chong, J. H., Shum, P., Haryono, H., Yohana, A., Rao, M. K., Lu, C., and Zhu, Y., "Measurements of refractive index sensitivity using long-period grating refractometer," *Optics Communications*, 229, 65-69 (2004).
- [10] Ishaq, I. M., Quintela, A., James, S. W., Ashwell, G. J., Lopez-Higuera, J. M., and Tatam, R. P., "Modification of the refractive index response of long period gratings using thin film overlays," *Sensors and Actuators B*, 107, 738-741 (2005).
- [11] Yang, J., Yang, L., Xu, C-Q., Xu, C., Huang, W., and Li, Y., "Long-period grating refractive index sensor with a modified cladding structure for large operational range and high sensitivity," *Applied Optics*, 45(24), 6142-6147 (2006).
- [12] Yang, X., Luo, S., Chen, Z., and Ng, J. H., "Refractive index sensor based on fiber laser," *Microwave and Optical Technology Letters*, 49(4), 916-918 (2007).
- [13] Jie Zeng, J., and Liang, D., "Application of fiber optic surface plasmon resonance sensor for measuring liquid refractive index," *Journal of Intelligent Material System and Structures*, 17, 787-791 (2006).
- [14] Banerjee, A., Mukherjee, S., Verma, R. K., Jana, B., Khan, T. K., Chakroborty, M., Das, R., Biswas, S., Saxena, A., Singh, V., Hallen, R. M., Rajput, R. S., Tewari, P., Kumar, S., Saxena, V., Ghosh, A. K., John, J., and Gupta-Bhaya, P., "Fiber optic sensing of liquid refractive index," *Sensors and Actuators B*, 123, 594-605, (2007).
- [15] Chaudhari, A. L., and Shaligram, A. D., "Multi-wavelength optical fiber liquid refractometry based on intensity modulation," *Sensors and Actuators A*, 100, 160-164 (2002).
- [16] Ni, N., Chan, C. C., Xia, L., and Shum, P., "Fiber cavity ring-down refractive index sensor," *IEEE Photonics Technology Letters*, 20(16), 1351-1353 (2008).
- [17] Martelli, C., Canning, J., Kristensen, M., and Grothoff, N., "Refractive index measurement within a photonic crystal fibre based on short wavelength diffraction," *Sensors*, 7, 2492-2498 (2007).